High-accuracy profiler that uses depth from focus

Paul W. Fieguth and David H. Staelin

A CCD-based confocal microscope system that is used to measure accurate three-dimensional surface profiles is reported. For a field of view of 500 μm, surface samples spaced at 12 μm on smooth specular test objects are simultaneously resolved in depth to ~1 μm (depending on the surface being observed). A precision of 0.1 μm is obtained for a mirrored surface for a field of view 400 μm wide. Simple scaling and sampling results permit these results to be extended to other apparatus dimensions and range sampling intervals.

Introduction

Recent advances in manufacturing have motivated interest in automated quality control, which may require routine quantitative inspection of an object's three-dimensional shape or profile. Useful profiling system characteristics sought here include speed, accuracy, and generality to various materials and scales of observation. The same characteristics are desired when one-of-a-kind objects are measured for analysis, repair, or duplication. One representative application of such a profiling system is the inspection to near-micrometer accuracy of computer-generated prototypes (for example, any of the metal or ceramic deposition prototyping systems currently under development). The confocal microscope arrangement[1] (originally the tandem-scanning microscope[2]) has been the object of considerable research effort[3–5] and is well suited to the prototype inspection task; since the illumination and the observation beams share a common path, such a system is less subject to some of the shadowing or masking problems common to competing surface profiling schemes that use triangulation or wide-angle interferometry.

This apparatus was not developed as a practical industrial tool. Our purpose in this research was to assess the limits of accuracy of the proposed profiling system. No effort was made to achieve practical computational times with the understanding that faster computation could be realized by parallelization, dedicated hardware, or approximated algorithms.

The authors are with the Research Laboratory of Electronics, Massachusetts Institute of Technology, Cambridge, Massachusetts 02139.

Received 25 March 1993; revision received 16 June 1993.
0003-6935/94/040686-04$06.00/0.

Apparatus

Most confocal scanning microscopes place an array of pinholes between the light source and the sample[3]; such a construction requires intense light, frequently an arc light or a laser, for adequately illuminating the sample. One novelty of our apparatus is in the use of an array of holes larger than pinholes (i.e., the radius of the image of the hole projected into the sample exceeds the Airy radius of the imaging lens), which permits the use of a simple 12-V bulb for illumination.

Common confocal profiling systems employ a servomechanism to determine profile samples one point at a time, with the accuracy limited only by the depth of focus. Because our apparatus profiles a whole field of view in parallel, we do not have the luxury of sampling the range axis at arbitrary points (as in the case of a servosystem); rather, we sample at uniform intervals in range and estimate the entire profile from these samples.

The microscope apparatus is shown in Fig. 1, where $d_{obj} = 1$ cm, $d_{lens} = 5$ mm, and $d_{image} = d_{pattern} = 17$ cm. Incandescent light is concentrated on a pattern on a 35-mm slide; the slide image is a regular array of transparent disks (of diameter 40 μm; disk centers are spaced ~100 μm apart). The pattern image is projected through a microscope objective (10×, numerical aperture 0.25) onto the object under study. The object is then imaged by a standard 512 × 480 National Television System Committee CCD camera (with an attached long-range microscope that permits a greater camera standoff distance of ≈35 cm). The object is mounted on a four-axis stage (three linear axes and one rotational axis); the position along each linear axis is set by stepper motors in 2.5-μm steps. Since stepper motors move the object in discrete steps, the position of the object at any point in time is known by counting (integrating) motor steps.

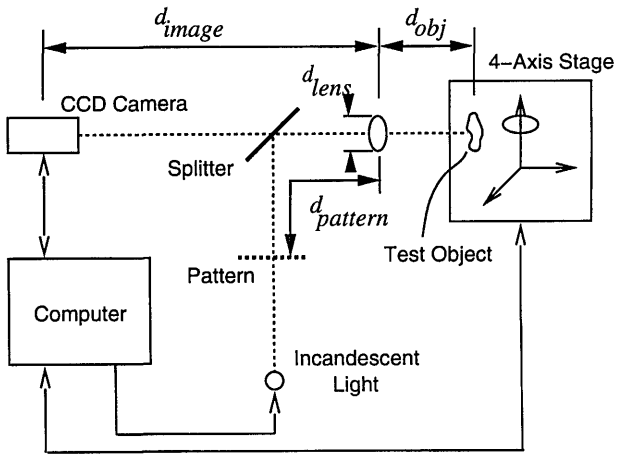

Fig. 1. Confocal microscope configuration with incandescent illumination and CCD detection.

Profile Estimation

One surface depth estimate is prepared for each of the approximately 650 projected disks within the field of view of the CCD (the field of view is slightly less than 0.5 mm on a side). A significant advantage of the use of a CCD array is that object depth can in principle be estimated at many points simultaneously, with processing delay reductions of the order of 600 possible, in principle, relative to single-spot systems. Further apparatus details may be found in the references.[6]

To obtain a surface profile, the object under study is scanned unidirectionally through the confocal microscope's depth of field along the Z axis in steps of δ_z. At each distance z, M CCD frames are captured and averaged; for the $N \times N$ pixel image surrounding each projected disk d, a quantitative measure of focus $f(z, d)$ is calculated and stored. Finally, the depth offset corresponding to disk d is estimated by comparing the ensemble $f(z, d)$ with a focus calibration function $c(z)$. In our experiments, $N = 16$; the value of M varied between 1 and 10, depending on the diffusivity of the material being studied. The following three paragraphs discuss and clarify these steps; considerable elaboration may be found in Ref. 6.

In a typical confocal microscope system, the focus measure $f(z, d)$ equals the intensity of illumination at a pinhole detector. Because we project relatively large disks onto the sample, the depth of focus, based on the intensity at the observed center of the disk, is increased. As a result, we do not base $f(z, d)$ purely on the intensity at a single pixel; instead, since defocusing is basically a spatial low-pass filtering operation, a reasonable shift-invariant quantitative focus measure may be computed as a weighted mean of discrete-Fourier-transform coefficient energies. That is, for the local $N \times N$ ($N = 16$) pixel region with brightness $p_{z,d}(x, y)$ centered on pattern disk d, the associated focus measure $f(z, d)$ can be given by

$$f(z, d) = \sum_{k_x=0}^{N-1} \sum_{k_y=0}^{N-1} \beta(k_x, k_y) \| P_{z,d}(k_x, k_y) \|^2 \qquad (1)$$

for some weighting $\beta(\,)$, where $P_{z,d}(\,)$ is the discrete Fourier transform of $p_{z,d}(\,)$. To avoid prohibitively long processing times, an approximate specific case of Eq. (1) that is calculable in the spatial domain is preferred:

$$f(z, d) = \sum_{x=0}^{N-1} \sum_{y=0}^{N-2} \{[p_{z,d}(x, y) - p_{z,d}(x, y + 1)]^2 + [p_{z,d}(x, y) - p_{z,d}(x + 1, y)]^2\}. \qquad (2)$$

To avoid energy spillover from the $N \times N$ region associated with one spot to neighboring regions, the location of each projected spot is detected and centered within its region (which prevents a spot from straddling the edge of an $N \times N$ region).

Figure 2 shows a representative focus measure obtained by the use of Eq. (2) with a mirror as a test object. The asymmetry in the curve is due to thick-lens effects (these effects have been demonstrated by ray tracing). The calibration function $c(z)$, which is densely sampled in z and interpolated to be continuous, is determined as the average of an ensemble of observed $f(z, d)$ curves from an ideal (e.g., mirrored) surface. As discussed below, to remove variations in the pattern from one spot to another, we may determine separate calibration functions $c_d(z)$ for each spot.

Without further knowledge of the surface being analyzed, a maximum-likelihood (ML) detector is optimal; a pseudo-ML estimator is implemented as follows for a given calibration $c(z)$ and observed $f(z, d)$ focus curves:

$$\hat{\Delta}_d = \arg_\Delta \max\left[\sum_n c(n\delta_z - \Delta) f(n\delta_z, d)\right], \qquad (3)$$

$$\hat{\alpha}_d = \left[\sum_n c(n\delta_z - \hat{\Delta}_d) f(n\delta_z, d)\right] \Big/ \sum_n c^2(n\delta_z - \hat{\Delta}_d), \qquad (4)$$

$$\overline{\Delta}_d = \arg_{\Delta \approx \hat{\Delta}_d} \min \sum_n [\hat{\alpha}_d c(n\delta_z - \Delta) - f(n\delta_z, d)]^2, \qquad (5)$$

that is, $\hat{\Delta}_d$ [Eq. (3)] is a coarse depth estimate that is

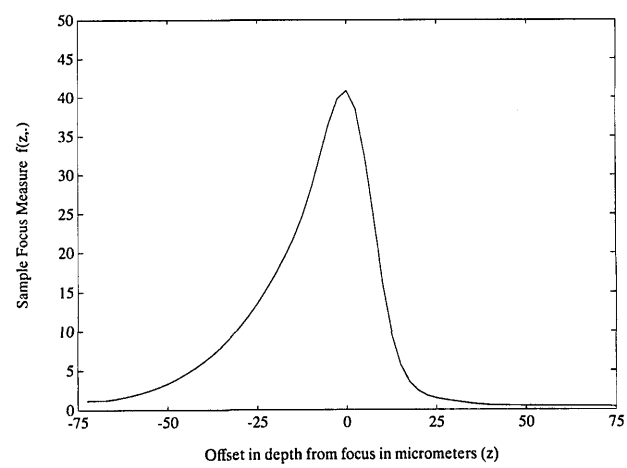

Fig. 2. Typical observed blur data with a mirror as the test object.

made by using correlation (i.e., discrete time-matched filtering), and $\hat{\alpha}_d$ is the estimated multiplicative scaling factor between $c(\,)$ and $f(.,d)$. $\overline{\Delta}_d$ is the refined depth estimate of range corresponding to disk d. The estimator fails to be ML to the extent that the scaling factor α is estimated rather than known exactly. The summation of Eq. (5) is a declining measure of the estimate confidence [i.e., the degree of congruence between signal $f(z, d)$ and matched filter $c(z)$] and can be used in postprocessing to flag unreliable depth estimates. The form of the ML estimator in Eq. (3) assumes white additive noise; in empirical tests, the difference signal $f(z, d) - c(z)$ is predominantly white,[6] which justifies this assumption. For small M, the noise of $f(z, d)$ is dominated by the white CCD pixel noise.

Results

We have expended minimal effort to optimize the profiling time; however, a sample set of times is included for the interested reader. In the following example, $M = 2$ CCD images were sampled at each of 60 positions of range:

- Sampling, 25 s;
- Frame averaging, 335 s;
- $f(z, d)$ calculation, 395 s;
- Estimation, 48 s.

All times are proportional to the number of range samples; the frame averaging time is also proportional to M. As most of our calculations are performed in floating point for convenience, at the very least the potential exists for significant improvements in speed when a fixed point is used.

Table 1 lists the error levels observed for six test cases; the achieved accuracies are competitive with profilers operating at a similar scale.[7] M refers to the number of CCD frames averaged (averaging reduces CCD pixel variance). A single calibration curve (or matched filter) $c(z)$ may be used for all pattern disks; this is denoted by group calibration. Alternatively, at the expense of computer memory use, a separate curve $c_d(z)$ may be determined for each pattern spot; this is denoted by individual calibration. Individual calibration reduces the effect of variations between spots over the pattern; a higher-quality pattern would eliminate this need.

For the purposes of determining estimator precision, the test object is assumed to be flat. Since the test objects may not be perfectly flat, the reported errors include a component originating from test object curvature. To remove the uncertainty caused by test object shape, a repeatability test can be performed, in which the reported error is based on the difference between successive profiles of the same point on the object. Repeatability errors, which form a lower bound on attainable accuracy, are ~0.03 μm rms when a mirror is used as the test object.

Significant differences in profiling accuracy can be attributed to surface nonuniformities, which are present on a micrometer scale, of the objects being observed. There are at least two microeffects of interest: surface light diffusion and microfacet reflection. For a diffuse surface, the incident light penetrates the surface and smears, effectively applying a low-pass filter to the projected pattern, and thereby reducing the signal-to-noise ratio; this effect is quite noticeable in chalk and plastics. For microcrystalline surfaces (e.g., metals), the surface may be modeled as a large collection of tiny reflections whose surface normal is a random vector; these facets cause glinting (i.e, bright spots outside the projected disk or dark spots within it), which changes the observed image and degrades the matched filter fit.

Figure 3 shows the depth error values corresponding to the third row of Table 1 (i.e., mirror test object, individual calibration, extensive CCD pixel averaging). Four of the greatest estimation errors (i.e., deviations from an estimate of 0.0) coincide with defects in the projected pattern; in principle, these could readily be eliminated with superior pattern slides.

Since our primary goal in this research is to establish limits of accuracy for our apparatus, tests on flat surfaces are sufficient to meet this end. Meaningful quantitative remarks are difficult to make regarding the profiles of irregular or rough surfaces because the exact profile is unknown. A variety of edge profiles, from 2 to 50 μm in height and 0 to 50 μm in width, have been measured; the profiling

Table 1. Profiling Accuracies for Various Test Cases

Test Object	CCD Frames M	Calibration	Error Std. Dev. (μm)
Mirror	1	Group	0.2
Mirror	5	Group	0.13
Mirror	5	Indiv.	0.08
Plastic (microchip)	5	Indiv.	1.0
Chalk	5	Indiv.	1.5
Copper (penny)	5	Indiv.	2.0

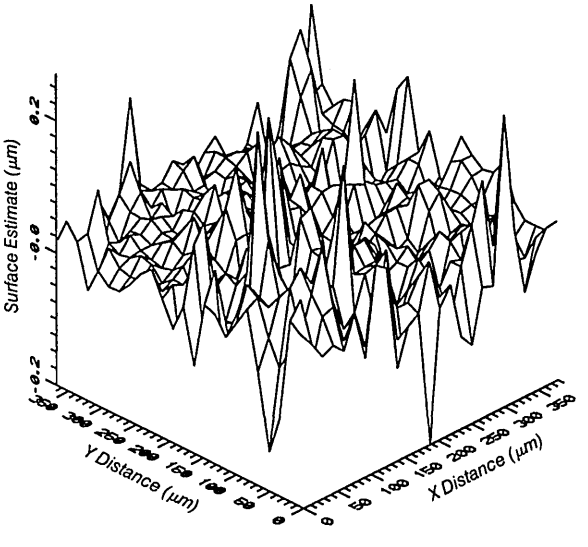

Fig. 3. Profiling error for a mirrored surface (row 3 of Table 1).

errors of the piecewise flat areas are consistent with those in Table 1.

The discussion thus far has been limited to sampling along a range as finely as possible ($\delta_z = 2.5$ μm). In practical applications, to improve the profiling rate (or to scan over a greater depth range), larger steps would be preferred. An approximate form of the error dependence on δ_z is easy to derive given the following assumptions: the calibration curve $c(z)$ is finely sampled relative to all values of δ_z of interest, the number of sampled images remains constant, δ_z is smaller than the depth of focus, and the noise is predominantly additive and white. Under these conditions, the estimation error is proportional to $\sqrt{\delta_z}$. An increase in δ_z from 2.5 to 10 μm resulted in a doubling of the incurred error; the error increased rapidly for δ_z in excess of 10 μm.

As our focus measure is a function of the classical point-spread function radius (rather than the diffraction intensity function) over range, the scaling of profiling accuracy with respect to the apparatus parameters in Fig. 1 is different from that in Ref. 8. Assuming that a classical thin-lens description of the system is adequate (i.e., d_{lens} is sufficiently large and d_{image} is sufficiently small so that the projected pattern is not diffraction dominated), then the profiling error is inversely proportional to the rate of increase of the point-spread function radius (as seen by the camera) with range. Let δ represent the offset along the range axis from the focus of a mirror being swept along the range axis:

$$\left.\frac{\text{Blur Radius}}{\delta}\right|_{\delta=0} \propto \frac{d_{\text{lens}} d_{\text{image}}}{d_{\text{obj}}^2}, \tag{6}$$

where the dimensions are defined in Fig. 1; d_{obj} is the distance from the objective lens to the test object, d_{lens} is the objective lens diameter, and d_{image} is the distance to the imaging camera. This permits earlier rms accuracy results to be approximately scaled for other apparatus dimensions.

In conclusion, a surface profiling system has been demonstrated with a confocal microscope and a CCD array detector capable of depth measurements accurate to less than 0.5 μm on a field of view of 400 μm.

The support of the Natural Sciences and Engineering Research Council of Canada and the Massachusetts Institute of Technology Leaders for Manufacturing Program is gratefully acknowledged.

References

1. T. Wilson and C. Sheppard, *Theory and Practice of Scanning Optical Microscopy* (Academic, New York, 1984).
2. M. Petran, M. Hadravsky, M. D. Egger, and R. Galambos, "Tandem-scanning reflected-light microscope," J. Opt. Soc. Am. **58,** 661–664 (1968).
3. G. S. Kino and T. R. Corle, "Confocal scanning optical microscopy," Phys. Today **42,** 55–62 (1989).
4. T. Wilson, "Imaging properties and applications of scanning optical microscopes," Appl. Phys. **22,** 119–128 (1980).
5. G. Q. Xiao, T. R. Corle, and G. S. Kino, "Real-time confocal optical scanning microscope," Appl. Phys. Lett. **53,** 716–718 (1988).
6. P. W. Fieguth, "Range estimation accuracy using depth-from-focus methods—theory and experiment," M.S. thesis (Massachusetts Institute of Technology, Cambridge, Mass., 1992).
7. M. H. Tulloch, "Accent on applications," Photon. Spectra **26**(3), 18–20 (1992).
8. T. R. Corle, C. H. Chou, and G. S. Kino, "Depth response of confocal optical microscopes," Opt. Lett. **11,** 770–772 (1986).